

The twist-three distribution $e^q(x, k_\perp)$ in a light-front model

Barbara Pasquini^{1,2,*} and Simone Rodini^{1,2,†}

¹*Dipartimento di Fisica, Università degli Studi di Pavia, I-27100 Pavia, Italy*

²*Istituto Nazionale di Fisica Nucleare, Sezione di Pavia, I-27100 Pavia, Italy*

(Dated: August 10, 2018)

We discuss the twist-three, unpolarized, chiral-odd, transverse momentum dependent parton distribution (TMD) $e^q(x, k_\perp)$ within a light-front model. We review a model-independent decomposition of this TMD, which follows from the QCD equations of motion and is given in terms of a leading-twist mass term, a pure interaction-dependent contribution, and singular terms. The leading-twist and pure twist-three terms are represented in terms of overlap of light-front wave functions (LFWFs), taking into account the Fock states with three valence quark ($3q$) and three-quark plus one gluon ($3q + g$). The $3q$ and $3q + g$ LFWFs with total orbital angular momentum zero are modeled using a parametrization derived from the conformal expansion of the proton distribution amplitudes, with parameters fitted to reproduce available phenomenological information on the unpolarized leading-twist quark and gluon collinear parton distributions. Numerical predictions for both the quark TMD $e^q(x, k_\perp)$ and the collinear parton distribution $e^q(x)$ are presented, discussing the role of the quark-gluon correlations in the proton.

I. INTRODUCTION

Higher-twist parton distributions, especially when the dependence on the parton transverse momenta is taken into account, give access to a wealth of information about the nucleon parton structure [1–3]. They describe multiparton correlations inside the nucleon, corresponding to the interference between scattering from a coherent quark-gluon pair and from a single quark [4–7]. As such, they help understanding the quark-gluon dynamics inside the hadrons, and go beyond the probabilistic interpretation that applies to the leading-twist parton distribution functions.

Twist-three parton distributions functions (PDFs) and transverse momentum dependent parton distributions (TMDs) contribute to various observables in inclusive and semi-inclusive deep inelastic scattering (SIDIS), respectively. Although suppressed with respect to twist-two observables, twist-three structure functions are not small in the kinematics of fixed target experiments. One of the priority tasks of the future experimental program at JLab12 is the measurement of different higher-twist spin-azimuthal asymmetries in SIDIS [8–10]. A future electron ion collider would extend such experimental investigation by accessing different kinematical regions [11, 12].

In this context, model studies have been shown to have important impact for the understanding of TMDs and the theoretical interpretation of related observables (see, e.g., Ref. [13]). Higher-twist quark PDFs and TMDs can in general be decomposed into contributions from leading-twist mass terms, singular terms and pure interaction-dependent (“tilde”) terms. This decomposition is obtained through the QCD equations of motion (EOM) and allows one to single the tilde term out as the contribution of quark-gluon correlation functions. Neglecting the tilde and mass terms is referred to as Wandzura-Wilczek approximation [14]. This approximation has been often used as starting point to simplify the description of twist-three SIDIS observables [15–17], and showed to be an useful numerical approximation [18]. However, there is no real experimental evidence of its validity, and it misses one of the main motivation to study sub-leading twist, i.e. the non-perturbative physics of quark-gluon correlations.

Twist-three TMDs have been calculated in various models: the MIT bag model [4, 19–21], diquark spectator models [22–25], instanton models of QCD vacuum [26, 27], chiral quark soliton models [28–32] and perturbative light-front Hamiltonian approaches with a quark target [33–36]. Although quark models do not have explicit gluon degrees of freedom, they describe interacting quarks and can generate non-vanishing tilde terms [21, 37].

In this work we want to make a step forward with respect to quark-model calculations and take into account explicitly the contribution from intrinsic gluon degrees of freedom. To this aim, we use the language of light-front wave functions

*Electronic address: barbara.pasquini@pv.infn.it

†Electronic address: simone.rodini01@ateneopv.it

(LFWFs), that provide a convenient framework for modelling parton distribution functions [38–40]. We focus on the twist-three, unpolarized, chiral-odd quark TMD $e^q(x, k_\perp)$ [6], which is constructed as overlap integrals between LFWFs with the minimum (valence) and next-to-minimum (one extra gluon) parton content. The LFWFs are modeled in the same spirit of Ref. [41], where the calculation was restricted to the leading-twist PDFs and to the twist-three polarized structure function $g_2^q(x)$. In particular, we consider only the Fock states with zero partons' orbital angular momentum, which are expected to be the dominant contribution for unpolarized distribution functions. These LFWF components for the $3q$ and $3q + g$ Fock states are related, in the light-front limit (zero transverse separation), to the nucleon twist-three and twist-four distribution amplitudes (DAs), respectively. We then use the lattice and QCD sum rule results for the proton DAs as guideline to parametrize the dependence of the LFWFs on the longitudinal momenta of the partons. For the dependence on the partons' transverse momentum k_\perp we adopt a Gaussian form, modified according to the Brodsky-Huang-Lepage prescription [42] to take into account a non-vanishing mass of the partons. The mass of the partons along with the other parameters modelling the proton DAs are then fitted to reproduce the results for the quark and gluon unpolarized twist-two PDFs from available phenomenological parametrizations. Having specified the LFWFs, we calculate the $e^q(x, k_\perp)$ TMD and $e^q(x)$ PDF, discussing the role of the twist-two and the genuine twist-three contributions, and compare our predictions with available phenomenological information.

The work is organized as follows: in Sec. II we introduce the definitions of the unpolarized twist-two TMDs of quark and gluon $f_1^{q/g}(x, k_\perp)$ and the twist-three quark TMD $e^q(x, k_\perp)$, and we review the general decomposition of $e^q(x, k_\perp)$ derived from the QCD EOM. In Sec. III, we present the Fock-state expansion of the proton state, and describe a model-independent representation of the LFWFs for the $3q$ and $3q + g$ components with zero partons' orbital angular momentum, as derived originally in Refs. [41, 43]. Then, we construct the corresponding LFWF overlap representation for the pure twist-three contribution to $e^q(x, k_\perp)$ and introduce our parametrization for the LFWFs, in terms of proton DAs. In Sec. IV, we fix the model parameters of the LFWFs by fitting the quark and gluon PDF $f_1(x)$ to the MMHT2014 parametrization [44] at the scale of 1 GeV^2 , and discuss our model predictions for both the TMD $e^q(x, k_\perp)$ and the PDF $e^q(x)$. We summarize the work in Sec. IV C. Technical details about the derivation of the model-independent decomposition of e^q are given in App. A, and the expression of $e^q(x, k_\perp)$ in terms of our model LFWFs can be found in App. B.

II. DEFINITION OF UNPOLARIZED DISTRIBUTIONS AND DECOMPOSITION OF $e^q(x, k_\perp)$

Quark TMDs are defined from the twist expansion of the following quark-quark correlators (see, e.g., Refs. [3, 45]).

$$\Phi^q(x, k_\perp, S) = \int \frac{dz^- dz_\perp}{(2\pi)^3} e^{iz^- k^+ - iz_\perp \cdot k_\perp} \langle P, S | \bar{\psi}(0) \mathcal{W}(0; z) \psi(z) | P, S \rangle |_{z^+=0}, \quad (1)$$

with $k^+ = xP^+$ ¹. The target state is characterized by its four-momentum P and the covariant spin vector S . In Eq. (1), ψ is the quark field and \mathcal{W} is an appropriate Wilson line, that connects the bilocal quark operators and ensures gauge invariance [46]. It is defined as:

$$\begin{aligned} \mathcal{W}(0, z) = & [0^+, 0^-, \mathbf{0}_\perp; 0^+, \infty^-, \mathbf{0}_\perp] \times [0^+, \infty^-, \mathbf{0}_\perp; z^+, \infty^-, \infty_\perp] \\ & \times [z^+, \infty^-, \infty_\perp; z^+, \infty^-, \mathbf{z}_\perp] \times [z^+, \infty^-, \mathbf{z}_\perp; z^+, z^-, \mathbf{z}_\perp] \end{aligned} \quad (2)$$

where $[a^+, a^-, \mathbf{a}_\perp; b^+, b^-, \mathbf{b}_\perp]$ denotes a gauge link connecting the points $a^\mu = (a^+, a^-, \mathbf{a}_\perp)$ and $b^\mu = (b^+, b^-, \mathbf{b}_\perp)$ along a straight line.

At twist-three level, we find three unpolarized T-even quark TMDs, i.e. the twist-two TMD $f_1^q(x, k_\perp)$, and the twist-three TMDs $e^q(x, k_\perp)$ and $f^\perp(x, k_\perp)$. In the following, we restrict ourselves to discussing the TMDs f_1 and e , which do not involve partons' orbital angular momentum transfer between the initial and final states. They are defined in terms of the quark-quark correlator as

$$f_1^q(x, k_\perp) = \Phi^{[\gamma^+]} = \frac{1}{2} \int dk^- \text{tr}[\Phi^q \gamma^+] = \int \frac{dz^- d^2 z_\perp}{2(2\pi)^3} e^{ik \cdot z} \langle P | \bar{\psi}(0) \mathcal{W}(0; z) \gamma^+ \psi(z) | P \rangle |_{z^+=0}, \quad (3)$$

¹ We use light-front coordinates, with $v^\pm = \frac{1}{\sqrt{2}}(v^0 \pm v^3)$ and $\mathbf{v}_\perp = (v^1, v^2)$ for a generic four-vector v .

$$\frac{M}{P^+} e^q(x, k_\perp) = \Phi^{[1]} = \frac{1}{2} \int dk^- \text{tr}[\Phi^q \mathbb{1}] = \int \frac{dz^- d^2 z_\perp}{2(2\pi)^3} e^{ik \cdot z} \langle P | \bar{\psi}(0) \mathcal{W}(0; z) \mathbb{1} \psi(z) | P \rangle |_{z^+=0}, \quad (4)$$

where $\langle P | \dots | P \rangle$ denotes the target spin-averaged matrix element and M is the nucleon mass. The quark collinear PDFs $f_1^q(x)$ and $e^q(x)$ are obtained by integrating the corresponding TMDs over the transverse momentum \mathbf{k}_\perp .

For later convenience, we also introduce the gluon unpolarized twist-two PDF $f_1^g(x)$, defined in terms of the gluon correlator $\Phi^{g,ji}(x, \mathbf{k}_\perp)$ as

$$f_1^g(x, k_\perp) = -g_{ij} \Phi^{g,ji}(x, k_\perp) = \sum_{a=1}^8 \sum_{i=1}^2 \frac{1}{xP^+} \int \frac{dz^- dz_\perp}{(2\pi)^3} e^{ik \cdot z} \langle P, S | \mathcal{W}(z; 0) F_a^{+i}(0) \mathcal{W}(0; z) F_a^{+i}(z) | P, S \rangle |_{z^+=0}, \quad (5)$$

where $F_a^{\mu\nu}$ is the gluon field strength tensor and a is the color index.

We now focus our attention on the quark TMD $e^q(x, k_\perp)$, and review its general decomposition in terms of leading-twist quark-mass terms, singular terms and pure interaction-dependent contributions. The bilocal quark operator entering the definition in Eq. (4) can be rewritten as

$$\mathcal{O}(0; z^-, \mathbf{z}_\perp) = \bar{\psi}(0) \mathcal{W}(0; z) \psi(z) |_{z^+=0} = \bar{\psi}_+(0) \mathcal{W}(0; z) \psi_-(z) |_{z^+=0} + \bar{\psi}_-(0) \mathcal{W}(0; z) \psi_+(z) |_{z^+=0}, \quad (6)$$

where we introduced the projection of the quark fields into the light-cone ‘good’ and ‘bad’ components, i.e., $\psi_+ = \mathcal{P}^+ \psi = \psi_+$ and $\psi_- = \mathcal{P}^- \psi$, respectively, with $\mathcal{P}^\pm = \frac{1}{2} \gamma^\mp \gamma^\pm$. The bad component ψ_- is a constrained field, as follows from the QCD EOM:

$$iD^+ \psi_-(z) = \frac{\gamma^+}{2} (i\boldsymbol{\gamma}_\perp \cdot \mathbf{D}_\perp + m) \psi_+(z), \quad (7)$$

where the covariant derivative is defined as

$$D^\mu = \partial^\mu - ig_s A^\mu, \quad (8)$$

with g_s the strong coupling constant. If we assume that the plus component k^+ of the quark’s momentum is strictly positive, we can invert the EOM (7) in a straightforward way using the Fourier expansion of the fields. Instead, problems arise when we include the contribution from zero modes corresponding to $k^+ = 0$. In this case, there appear singularities in the bad components of the field, and one needs a regularization prescription [47, 48]. To this aim, we follow the procedure outlined in Refs. [6, 49] and use the EOM (7) to derive the following operator identity

$$\begin{aligned} \mathcal{W}(0; z) \psi_-(z) |_{z^+=0} &= \mathcal{W}_1(0^-, \mathbf{0}_\perp; 0^-, \mathbf{z}_\perp) \psi_-(0^+, 0^-, \mathbf{z}_\perp) \\ &\quad - i \int_0^{z^-} d\zeta^- \mathcal{W}_1(0^-, \mathbf{0}_\perp; \zeta^-, \mathbf{z}_\perp) \frac{\gamma^+}{2} (i\boldsymbol{\gamma}_\perp \cdot \mathbf{D}_\perp + m) \psi_+(0^+, \zeta^-, \mathbf{z}_\perp), \end{aligned} \quad (9)$$

where we defined $\mathcal{W}_1(a^-, \mathbf{a}_\perp; b^-, \mathbf{b}_\perp) \equiv \mathcal{W}(0^+, a^-, \mathbf{a}_\perp; 0^+, b^-, \mathbf{b}_\perp)$. Using the expression in Eq. (9) for the bad component, Eq. (6) can be rewritten as

$$\mathcal{O}(0; z^-, \mathbf{z}_\perp) = \mathcal{O}_s + \mathcal{O}_m + \mathcal{O}_{\text{tw}3}, \quad (10)$$

with

$$\mathcal{O}_s = \bar{\psi}(0) \mathcal{W}_1(0^-, \mathbf{0}_\perp; 0^-, \mathbf{z}_\perp) \psi(0^+, 0^-, \mathbf{z}_\perp), \quad (11)$$

$$\mathcal{O}_m = -im \int_0^{z^-} d\zeta^- \bar{\psi}_+(0) \mathcal{W}_1(0^-, \mathbf{0}_\perp; \zeta^-, \mathbf{z}_\perp) \gamma^+ \psi_+(0^+, \zeta^-, \mathbf{z}_\perp), \quad (12)$$

$$\mathcal{O}_{\text{tw}3} = -\frac{i}{2} \int_0^{z^-} d\zeta^- \bar{\psi}_+(0) \sigma^{j+} \left[\mathcal{W}_1(0^-, \mathbf{0}_\perp; \zeta^-, \mathbf{z}_\perp) \vec{D}_{\perp,j}(\zeta^-, \mathbf{z}_\perp) + \overleftarrow{D}_{\perp,j}(0) \mathcal{W}_1(0^-, \mathbf{0}_\perp; \zeta^-, \mathbf{z}_\perp) \right] \psi_+(0^+, \zeta^-, \mathbf{z}_\perp). \quad (13)$$

where the index $j = 1, 2$ labels the transverse component.

The bad components ψ_- contributes only to \mathcal{O}_s in Eq. (11). This operator, when inserted in the matrix element of Eq. (4) and integrated over z^- , gives a singular contribution proportional to $\delta(x)$:

$$e_s^q(x, k_\perp) = \frac{\delta(x)}{2M} \int \frac{dz_\perp}{(2\pi)^2} e^{-iz_\perp \cdot \mathbf{k}_\perp} \langle P | \bar{\psi}(0) \mathcal{W}_1(0^-, \mathbf{0}_\perp; 0^-, \mathbf{z}_\perp) \psi(0^+, 0^-, \mathbf{z}_\perp) | P \rangle. \quad (14)$$

This contribution is well known for the PDF $e^q(x)$, being related to the pion-nucleon-sigma term (see, e.g., Ref. [6]).

The contribution to e^q from the operator \mathcal{O}_m can be worked out using the Fourier expansion of the matrix element of the operator (12) and the definition of f_1^q in (3), as outlined in App. A, with the result

$$e_m^q = \frac{m}{Mx} f_1^q(x, k_\perp) - \frac{m}{M} \delta(x) \int_{-1}^1 dy \frac{f_1^q(y, k_\perp)}{y}, \quad (15)$$

where the singular term is a natural consequence of the divergences associated with the zero modes ($x = 0$).

Limiting ourselves to the T-even sector and to the target-spin averaged matrix element, the contribution from the operator \mathcal{O}_{tw3} can be rewritten as

$$\begin{aligned} e_{tw3} = & -\frac{P^+}{M} \frac{g_s}{2} \int \frac{dz^- dz_\perp}{2(2\pi)^3} e^{ik^+ z^- - \mathbf{k}_\perp \cdot \mathbf{z}_\perp} \\ & \times \left(\int_{0^-}^{z^-} d\zeta^- \int_{\infty^-}^{\zeta^-} d\eta^- \langle P | \bar{\psi}(0) \mathcal{W}_1(0^-, \mathbf{0}_\perp; \eta^-, \mathbf{z}_\perp) G_j^+(0^+, \eta^-, \mathbf{z}_\perp) \sigma^{j+} \mathcal{W}_1(\eta^-, \mathbf{z}_\perp; \zeta^-, \mathbf{z}_\perp) \psi(0^+, \zeta^-, \mathbf{z}_\perp) | P \rangle \right. \\ & \left. + \int_{0^-}^{z^-} d\zeta^- \int_{0^-}^{\infty^-} d\eta^- \langle P | \bar{\psi}(0) \mathcal{W}_1(0^-, \mathbf{0}_\perp; \eta^-, \mathbf{0}_\perp) G_j^+(0^+, \eta^-, \mathbf{0}_\perp) \sigma^{j+} \mathcal{W}_1(\eta^-, \mathbf{0}_\perp; \zeta^-, \mathbf{z}_\perp) \psi(0^+, \zeta^-, \mathbf{z}_\perp) | P \rangle \right), \end{aligned} \quad (16)$$

where $G^{\mu\nu}$ is the gluon field strength tensor. Using the results in App. A, Eq. (16) can be recast in the form

$$e_{tw3}^q(x, k_\perp) = \tilde{e}^q(x, k_\perp) - \delta(x) \int_{-1}^1 dy \tilde{e}^q(y, k_\perp), \quad (17)$$

where

$$\tilde{e}^q(x, k_\perp) = -\frac{i}{Mx} \Phi_{A,j}^{[\sigma^{j+}]}(x, k_\perp) \quad (18)$$

is a pure twist-three contribution defined in terms of the quark-gluon-quark correlation function [50]

$$\begin{aligned} \Phi_{A,j}^{[\sigma^{j+}]}(x, k_\perp) = & \frac{1}{2} \text{Tr} [\Phi_{A,j}(x, k_\perp) \sigma^{j+}] = \frac{g_s}{2} \int \frac{dz^- dz_\perp}{2(2\pi)^3} e^{ik^+ z^- - \mathbf{k}_\perp \cdot \mathbf{z}_\perp} \\ & \times \left(\int_{\infty^-}^{\zeta^-} d\eta^- \langle P | \bar{\psi}(0) \mathcal{W}_1(0^-, \mathbf{0}_\perp; \eta^-, \mathbf{z}_\perp) G_j^+(0^+, \eta^-, \mathbf{z}_\perp) \sigma^{j+} \mathcal{W}_1(\eta^-, \mathbf{z}_\perp; \zeta^-, \mathbf{z}_\perp) \psi(0^+, \zeta^-, \mathbf{z}_\perp) | P \rangle \right. \\ & \left. + \int_{0^-}^{\infty^-} d\eta^- \langle P | \bar{\psi}(0) \mathcal{W}_1(0^-, \mathbf{0}_\perp; \eta^-, \mathbf{0}_\perp) G_j^+(0^+, \eta^-, \mathbf{0}_\perp) \sigma^{j+} \mathcal{W}_1(\eta^-, \mathbf{0}_\perp; \zeta^-, \mathbf{z}_\perp) \psi(0^+, \zeta^-, \mathbf{z}_\perp) | P \rangle \right). \end{aligned} \quad (19)$$

Collecting the results in Eqs. (14)-(17), we end up with the following decomposition:

$$e^q(x, k_\perp) = e_s^q(x, k_\perp) + \tilde{e}^q(x, k_\perp) + \frac{m}{xM} f_1^q(x, k_\perp) - \delta(x) \int_{-1}^1 dy \left(\frac{m}{My} f_1^q(y, k_\perp) + \tilde{e}^q(y, k_\perp) \right). \quad (20)$$

The singular term beyond the contribution of e_s is usually not discussed in literature and, to the best of our knowledge, has never been written explicitly in this form.

The decomposition (20) is independent on the choice of the gauge. In the light-cone gauge $A^+ = 0$, with suitable boundary conditions at light-cone infinity for the transverse components of the gauge field, the gauge links in the correlators can be ignored and $\Phi_{A,j}$ in Eq. (19) is replaced by the following correlator [50, 51]

$$\tilde{\Phi}_{A,j}^{[\sigma^{j+}]}(x, k_\perp) = \frac{1}{2} \text{Tr} [\tilde{\Phi}_{A,j}(x, k_\perp) \sigma^{j+}] = \frac{g_s}{2} \int \frac{dz^- dz_\perp}{2(2\pi)^3} e^{ik \cdot z} \langle P, S | \bar{\psi}(0) [A_{\perp,j}(z) - A_{\perp,j}(0)] \sigma^{j+} \psi(z) | P, S \rangle_{z^+=0}. \quad (21)$$

In the framework of light-front quantization in the $A^+ = 0$ gauge, the effects of the final-state interactions associated with the gauge link can be reabsorbed in the LFWFs of the target, which acquire an imaginary phase [52]. As we are interested to T-even TMDs, these effects can be ignored, and in the following we will work only with real LFWFs.

Integrating Eq. (20) over \mathbf{k}_\perp , one obtains the corresponding decomposition for the PDF $e^q(x)$

$$e^q(x) = e_s(x) + \tilde{e}^q(x) + \frac{m}{xM} f_1^q(x) - \delta(x) \int_{-1}^1 dy \left(\frac{m}{My} f_1^q(y) + \tilde{e}^q(y) \right), \quad (22)$$

from which one can easily infer well-known relations for the first Mellin moments of $e^q(x)$ [6].

III. LIGHT-FRONT FOCK-STATE EXPANSION

In this section, we derive the LFWF overlap representation for the TMD $e^q(x, k_\perp)$. Since we will work under the assumption $k^+ > 0$, in the following we will not consider the singular terms in Eqs. (20) and (22).

In the framework of light-front quantization in the $A^+ = 0$ gauge, and restricting ourselves to the contributions from the $3q$ and $3q + g$ Fock-states, the light-front Fock-state expansion of a proton state with momentum P and light-front helicity Λ reads

$$|P, \Lambda\rangle = |P, \Lambda\rangle_{3q} + |P, \Lambda\rangle_{3q+g}, \quad (23)$$

with

$$|P, \Lambda\rangle_{3q} = \sum_{\{\lambda_i\}} \sum_{\{q_i\}} \int [Dx]_3 \Psi_{3q}^\Lambda(\beta, r) \varepsilon^{c_1 c_2 c_3} \prod_{i=1}^3 |\lambda_i, q_i, c_i, \tilde{k}_i\rangle, \quad (24)$$

$$|P, \Lambda\rangle_{3q+g} = \sum_{\{\lambda_i\}_{i=1}^4} \sum_{\{q_i\}} \int [Dx]_4 \Psi_{3q+g}^\Lambda(\beta, r) \varepsilon^{d c_2 c_3} T_{d, c_1}^a \left(\prod_{i=1}^3 |\lambda_i, q_i, c_i, \tilde{k}_i\rangle \right) |\lambda_4, g, a, k_i\rangle. \quad (25)$$

In Eqs. (24) and (25), Ψ_{3q}^Λ and Ψ_{3q+g}^Λ are, respectively, the LFWF for the $N = 3$ and $N = 4$ parton Fock state $\prod_{i=1}^N |\lambda_i, q_i, c_i, k_i\rangle$, with λ_i the parton light-front helicity, $q_i = u, d$ and g the quark and gluon flavor index, c_i the parton color index, and k_i the parton momentum. For the argument of the LFWFs, we used a collective notation, with $\beta = (\{\lambda_i\}; \{q_i\})$ and $r = \{\tilde{k}_i\}$, where $\tilde{k}_i = (k_i^+ = x_i P^+, \mathbf{k}_{\perp, i})$. Furthermore, the sum over the color indexes is understood, and, then, using also the sum over the flavor index, the color matrix in Eq. (25) can be saturated with the color index of the first quark only.

The integration measures are defined as:

$$[D\tilde{k}]_N = \frac{[dx]_N [d\mathbf{k}_\perp]_N}{\prod_{i=1}^N \sqrt{x_i}}, \quad (26)$$

$$[dx]_N = \delta \left(1 - \sum_{i=1}^N x_i \right) \prod_{i=1}^N dx_i, \quad (27)$$

$$[d\mathbf{k}_\perp]_N = \left(\frac{1}{2(2\pi)^3} \right)^{N-1} \delta^2 \left(\sum_{i=1}^N \mathbf{k}_{\perp, i} \right) \prod_{i=1}^N d\mathbf{k}_{\perp, i}. \quad (28)$$

The partial contribution of the N -parton Fock state is defined as

$${}_N \langle P' \Lambda' | P \Lambda \rangle_N = 2P^+ (2\pi)^3 \delta(P^+ - P'^+) \delta^2(\mathbf{P}'_\perp - \mathbf{P}_\perp) \delta_{\Lambda, \Lambda'} P_N, \quad (29)$$

where P_N is the probability to find the N -parton state in the proton.

Using the expressions of Eqs. (23)-(24) for the proton state in the definition (18), the LFWF overlap representation

of \tilde{e}^q reads

$$\begin{aligned}
\tilde{e}^q(x, \mathbf{k}_\perp) &= -\frac{\sqrt{2}g_s}{Mx} \int \frac{[d\tilde{\mathbf{k}}]_4}{\sqrt{x_4}} T_{d,c_1}^a \varepsilon^{dc_2c_3} \varepsilon^{c'_1c'_2c'_3} \sum_\Lambda \sum_{\{\lambda'_i\}} \sum_{\{q'_i\}} \sum_{\{\lambda_i\}} \sum_{\{q_i\}} \sum_{j,j'=1}^3 \delta_{q'_{j'},q} \delta_{q_j,q} \delta_{\lambda'_{j'},-\lambda_j} \delta_{\lambda_4,2\lambda'_{j'}} \\
&\times T_{c'_{j'},c_j}^a \left(\prod_{\substack{i=1 \\ i \neq j}}^3 \prod_{\substack{i'=1 \\ i' \neq j'}}^3 \delta_{c'_i,c_i} \delta_{q'_{i'},q_i} \delta_{\lambda'_{i'},\lambda_i} \right) \delta(x-x_j-x_4) \delta^2(\mathbf{k}_\perp - \mathbf{k}_{\perp,j} - \mathbf{k}_{\perp,4}) \\
&\times \Psi_{3q}^{\Lambda*} \left(\{\lambda'_i\}; \{q'_i\}; (\tilde{\mathbf{k}}'_{j'} = \tilde{\mathbf{k}}_j + \tilde{\mathbf{k}}_4); \{\tilde{\mathbf{k}}'_{i'} = \tilde{\mathbf{k}}_i\}_{i \neq j'} \right) \Psi_{3q+g}^\Lambda \left(\{\lambda_i\}; \{q_i\}; \{\tilde{\mathbf{k}}_i\} \right). \tag{30}
\end{aligned}$$

Eq. (30) involves the overlap of LFWFs for the $3q$ and the $3q+g$ Fock states, giving direct information on the quark-gluon correlations inside the proton. The momentum of the active quark in the $3q$ LFWF is set to the external momentum ($k^+ = xP^+, \mathbf{k}_\perp$) that is also the sum of the gluon momentum and one of the quark momentum in the $3q+g$ LFWF. This makes evident the partonic interpretation of the \tilde{e} term as an interference between scattering from a coherent quark-gluon pair and from a single quark [4–6].

The corresponding results for the LFWF overlap representation of the twist-two contribution to e^q , related to the unpolarized distribution f_1^q , are given in terms of the sum of the squares of the N -parton LFWFs, according to the density interpretation of the twist-two distributions (see, e.g., Ref. [53]).

A. Relation to nucleon distribution amplitudes

In this section, we present a parametrization of the proton LFWFs in terms of leading-twist (twist-three) and next-to-leading-twist (twist-four) proton DAs. To this aim, we consider the component of the proton state corresponding to vanishing total orbital angular momentum of the partons [41, 43, 54], i.e.²

$$|P, +\rangle_{3q}^{L_z=0} = \frac{-\varepsilon^{ijk}}{\sqrt{6}} \int [Dx]_{123} \Psi^{(0)}(1, 2, 3) \left(u_{\uparrow,i}^\dagger(1) u_{\downarrow,j}^\dagger(2) d_{\uparrow,k}^\dagger(3) - u_{\uparrow,i}^\dagger(1) d_{\downarrow,i}^\dagger(2) u_{\uparrow,k}^\dagger(3) \right) |0\rangle, \tag{31}$$

$$|P, +\rangle_{3q+g\downarrow}^{L_z=0} = \varepsilon^{ijk} \int [Dx]_{1234} \Psi^\downarrow(1, 2, 3, 4) T_{\sigma i g \downarrow}^a g_\downarrow^{a\dagger}(4) u_{\uparrow,\sigma}^\dagger(1) u_{\uparrow,j}^\dagger(2) d_{\uparrow,k}^\dagger(3) |0\rangle, \tag{32}$$

$$\begin{aligned}
|P, +\rangle_{3q+g\uparrow}^{L_z=0} &= \varepsilon^{ijk} \int [Dx]_{1234} \left[\Psi^{1\uparrow}(1, 2, 3, 4) T_{\sigma i g \uparrow}^a g_\uparrow^{a\dagger}(4) u_{\downarrow,\sigma}^\dagger(1) \left(u_{\uparrow,j}^\dagger(2) d_{\downarrow,k}^\dagger(3) - d_{\uparrow,j}^\dagger(2) u_{\downarrow,k}^\dagger(3) \right) \right. \\
&\quad \left. + \Psi^{2\uparrow}(1, 2, 3, 4) T_{\sigma j g \uparrow}^a g_\uparrow^{a\dagger}(4) u_{\downarrow,i}^\dagger(1) \left(u_{\downarrow,\sigma}^\dagger(2) d_{\uparrow,k}^\dagger(3) - d_{\downarrow,\sigma}^\dagger(2) u_{\uparrow,k}^\dagger(3) \right) \right] |0\rangle, \tag{33}
\end{aligned}$$

where g_\uparrow (g_\downarrow) denotes the gluon state with positive (negative) light-front helicity.

With respect to the expansion in terms of LFWFs of Eqs. (24) and (25), here the flavour and helicity structure of the parton composition is made explicit, and the light-front wave amplitudes (LFWAs) $\psi^{(j)}$ are scalar functions, which depend only on the parton momenta, i.e. the argument $i = 1, 2, 3, 4$ stands for $\tilde{\mathbf{k}}_i$. The dependence of the LFWAs on the factorization scale is implicit. The proton state with negative helicity is obtained from Eqs. (31)-(33) by applying the light-front parity transformation Y , which corresponds to a parity operation followed by a 180° rotation around the y axis. It acts on a state of momentum P and light-front helicity Λ as

$$Y|P\Lambda\rangle = (-1)^{s-\Lambda} \eta |P-\Lambda\rangle, \tag{34}$$

² In Ref. [43] one finds two LFWFAs for the $3q$ component with $L_z = 0$. However, one of them is suppressed, being related to a next-to-next to leading order DA, and will be neglected in the following.

where s is the total spin of the state and η is the intrinsic parity of the hadron ($\eta = +1$ for a proton and a quark state, $\eta = -1$ for a gluon state).

The representation of $\tilde{\epsilon}^g(x, k_\perp)$ in terms of overlap of the LFWAs in Eqs. (31)-(33) is reported in App. B. Following Ref. [41], we can write the LFWAs using the following factorized form

$$\Psi^{(0)}(1, 2, 3) = \frac{1}{4\sqrt{6}}\phi(x_1, x_2, x_3)\Omega_3(a_3, x_i, \mathbf{k}_{\perp,i}), \quad (35)$$

$$\Psi^\downarrow(1, 2, 3, 4) = \frac{1}{\sqrt{2x_4}}\phi_g(x_1, x_2, x_3, x_4)\Omega_4(a_\downarrow, x_i, \mathbf{k}_{\perp,i}), \quad (36)$$

$$\Psi^{1\uparrow}(1, 2, 3, 4) = \frac{1}{\sqrt{2x_4}}\psi^1(x_1, x_2, x_3, x_4)\Omega_4(a_\uparrow, x_i, \mathbf{k}_{\perp,i}), \quad (37)$$

$$\Psi^{2\uparrow}(1, 2, 3, 4) = \frac{1}{\sqrt{2x_4}}\psi^2(x_1, x_2, x_3, x_4)\Omega_4(a_\uparrow, x_i, \mathbf{k}_{\perp,i}), \quad (38)$$

where the \mathbf{k}_\perp -dependence of the functions Ω_N is assumed to be Gaussian, i.e.

$$\Omega_N(a_N, x_i, \mathbf{k}_{\perp,i}) = \frac{(16\pi^2 a_N^2)^{N-1}}{\prod_{i=1}^N x_i} \exp\left[-a_N^2 \sum_{i=1}^N \frac{k_{\perp,i}^2}{x_i}\right], \quad (39)$$

with the normalization:

$$\int [d\mathbf{k}_\perp]_{1\dots N} \Omega_N = 1. \quad (40)$$

The pure x_i -dependent part of the LFWAs in Eqs. (35)-(38) can be directly related to the proton DAs [38, 41, 55]. In particular, the LFWA which enters the $3q$ component of the proton state coincides with the leading twist-three proton DA, i.e.

$$\phi(x_1, x_2, x_3) = \Phi_3(x_1, x_2, x_3). \quad (41)$$

The LFWAs for $3q + g$ Fock-state are related to the next-to-leading-order twist-four DAs [56] by³

$$\phi_g(x_1, x_2, x_3, x_4) = \frac{M}{96g_s} (2\Xi_4^g(x_1, x_2, x_3, x_4) + \Xi_4^g(x_2, x_1, x_3, x_4)), \quad (42)$$

$$\psi^1(x_1, x_2, x_3, x_4) = -\frac{M}{96g_s} (2\Psi_4^g(x_2, x_1, x_3, x_4) + \Phi_4^g(x_1, x_2, x_3, x_4)), \quad (43)$$

$$\psi^2(x_1, x_2, x_3, x_4) = \frac{M}{96g_s} (2\Phi_4^g(x_1, x_2, x_3, x_4) + \Psi_4^g(x_2, x_1, x_3, x_4)). \quad (44)$$

The distribution amplitudes can be expanded into a basis of orthogonal polynomials, leaving all the factorization-scale dependence in the coefficients of the expansion. For the three-quark DA, we keep the first few terms of the conformal expansion, corresponding to [56]

$$\Phi_3(x_1, x_2, x_3) = 120f_N(\mu)x_1x_2x_3(1 + A(\mu)(x_1 - x_3) + B(\mu)(x_1 + x_3 - 2x_2)). \quad (45)$$

For the twist-four DAs, we adopt the asymptotic form, given by

$$\Xi_4^g(x_1, x_2, x_3, x_4) = \frac{8!}{6}x_1x_2x_3x_4^2\lambda_1^g(\mu), \quad (46)$$

$$\Psi_4^g(x_1, x_2, x_3, x_4) = \frac{8!}{4}x_1x_2x_3x_4^2\left(\lambda_2^g(\mu) + \frac{\lambda_3^g(\mu)}{3}\right), \quad (47)$$

$$\Phi_4^g(x_1, x_2, x_3, x_4) = -\frac{8!}{4}x_1x_2x_3x_4^2\left(\lambda_2^g(\mu) - \frac{\lambda_3^g(\mu)}{3}\right). \quad (48)$$

³ Eq. (42) differs by a sign from the corresponding relation in Ref. [41]. The opposite sign comes from using correctly the light-front parity transformation (34) to flip the light-front helicity of the partons, according to the definition of the Ξ_4^g DA.

The normalization constant $f_N(\mu)$ in Eq. (45) and the parameters $\lambda_i^g(\mu)$ of the expansion in Eqs. (46)-(48) have been evaluated using QCD sum rules [41] at the scale $\mu = 1$ GeV and in the chiral limit of vanishing quark masses, while the “shape” parameters A, B in Eq. (45) have been calculated on the lattice from the DA moments [57, 58].

In our approach, we introduce an explicit dependence on the mass of the “constituent” partons. This amounts to effectively taking into account the non-perturbative nature of the proton state modelled in terms of few Fock-state components. Accordingly, we use the Brodsky-Huang-Lepage prescription [42], and modify the \mathbf{k}_\perp -dependent part of the LFWA by replacing k_\perp^2 with $k_\perp^2 + m^2$, i.e., we use

$$\Omega_N(a_N, x_i, \mathbf{k}_{\perp,i}) = \frac{(16\pi^2 a_N^2)^{N-1}}{\prod_{i=1}^N x_i} \exp \left[-a_N^2 \sum_{i=1}^N \frac{k_{\perp,i}^2 + m_i^2}{x_i} \right]. \quad (49)$$

For the x -dependent part of the LFWAs, we keep the same expressions in terms of proton DAs as in Eqs (45)-(48). Since we moved away from the chiral limit, we do not use the results of QCD sum rule and lattice QCD for the coefficients of the DAs. Instead, we treat them as free parameters, as specified in the following.

IV. RESULTS

A. Fixing the parameters from twist-two parton distributions

The parameters of the LFWFs are fixed to reproduce available phenomenological parametrizations for the unpolarized PDF f_1 . In particular, we used the results of the MMHT2014 parametrization [44] at $Q^2 = 1$ GeV², i.e. the same scale of the results from lattice and QCD sum rules. The valence-quark contribution to f_1 is fitted in the range $x \in (0, 1)$, while we limit to $x \in (0.4, 1)$ for the fit of the gluon unpolarized PDF. In the last case, we did not include lower values of x , because in that region our nonperturbative constituent parton model is not able to catch the low- x dynamics of the gluons and, at the same time, the phenomenological parametrizations are not so well constrained at low x and low scales.

In the fit procedure, the renormalization constant f_N of the leading-twist DA in Eq. (45) and the parameters λ_1^g , λ_2^g and λ_3^g of the next-to-leading twist DAs in Eqs. (46)-(48) are considered to be distributed as Gaussian variables with means and standard deviations given by the estimates of the QCD sum rules and lattice calculations. The shape parameters A and B in Eq. (45) are sampled as uniform variables within a larger range than the error band of the lattice calculations. This allows us to having more flexibility to take into account the effects of finite quark and gluon masses. The parton masses along with the width of the \mathbf{k}_\perp distributions enter only in the parametrization of the functions Ω_N in Eq. (49). The parton masses are fitted with the constraint

$$0 \leq 3m_q + m_g \leq M. \quad (50)$$

Furthermore, we assume the same width for the k_\perp -distributions of the gluon with positive and negative helicity, i.e.

$$a_\downarrow = a_\uparrow = a_4, \quad (51)$$

and we take a_4 along with the width a_3 for the $3q$ state as additional free parameters. The fitted values of the coefficients of the leading-twist and next-to-leading-twist DAs are shown in Table I, in comparison with the values obtained from QCD sum rules in the chiral limit and lattice calculations. For the quark and gluon mass we obtain

$$m_q = 0.161 \text{ GeV}, \quad m_g = 0.050 \text{ GeV}. \quad (52)$$

For the widths, the fit results are

$$a_3 = 0.85 \text{ GeV}^{-1}, \quad a_4 = 0.92a_3, \quad (53)$$

which correspond to have a quark-gluon state slightly more compact in the transverse-momentum space as compared to the valence three-quark configuration.

We note that the two sets of parameters in Table I are consistent, within the uncertainty bands, except for the coefficients A and B . However, we found very small sensitivity of the fitted PDFs to the A and B parameters.

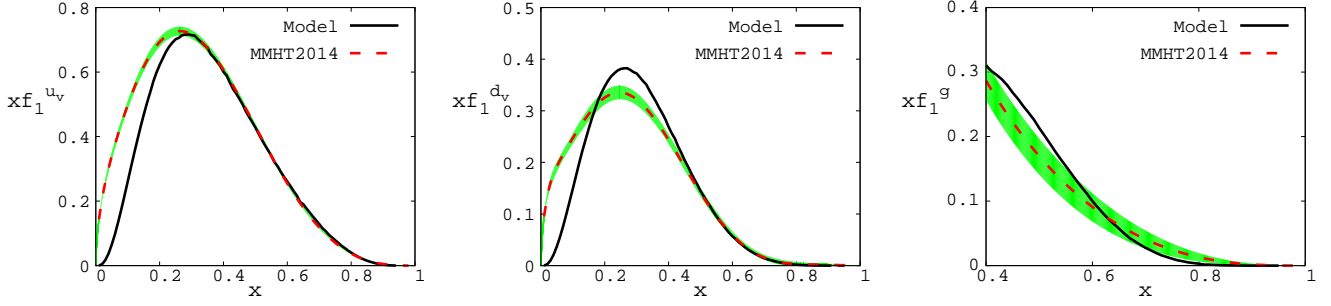


FIG. 1: The unpolarized PDF $xf_1(x)$ for the valence up-quark (left panel), for the valence down-quark (middle panel) and for the gluon (right panel) as function of x at $Q^2 = 1 \text{ GeV}^2$. Solid curve: results from the light-front model of this work, with the fit parameters in Table I and in Eqs. (52) and (53). Dashed curve: results from the parametrization of Ref. [44], with the corresponding uncertainty bands.

The fit results for the unpolarized parton distributions for the valence up and down quarks, and for the gluon are shown in Fig. 1, in comparison with the MMHT2014 phenomenological parametrizations [44] at $Q^2 = 1 \text{ GeV}^2$. The results for the quark PDFs reproduce very well the MMHT2014 parametrization at larger x (from $x \geq 0.2$, in the case of the up quark, and $x \geq 0.4$, for the down quark), while they have a much faster fall-off for $x \rightarrow 0$ than the Regge-motivated behavior of the parametrization. The results for the gluon PDF, in the fitted range of $x \geq 0.4$ reproduce well the MMHT2014 parametrization. Furthermore, for the probability of the $3q$ and $3q + g$ components of the proton state we find the following results

$$P_{3q} = 0.18, \quad (54)$$

$$P_{3q+g} = P_{3q+g\uparrow} + P_{3q+g\downarrow} = 0.38, \quad (55)$$

which are consistent with the values of Ref. [41].

B. Twist-three distributions

Using the explicit parametrization for the LFWAs given in Sec. IV A, and the LFWF overlap representation in App. B, we obtain the results shown in Figs. 2 for the PDF $xe^q(x)$ of up and down quarks. The red short-dashed curves show the contribution from the twist-two term, while the blue long-dashed curves correspond to the genuine twist-three contributions. The relative size of twist-two and genuine twist-three contributions depends on the quark-mass parameter, which enters as proportionality constant that weights the twist-two term in Eq. (22). In our model calculation, the partons' mass also enter the functions Ω_N in Eq. (49). However, in this case, the dependence on the partons' mass is such that it does not affect the relative size of the the twist-two and twist-three contributions to $xe^q(x)$, and slightly changes their behaviour as function of x .

We also note that the twist-two and genuine twist-three terms have a quite different x -dependence. The twist-two contribution is peaked at $x \approx 0.2$, with a fast fall-off at larger x , more pronounced in the case of up quarks than down

	$3q$			$3q + g$		
	f_N (10^{-3} GeV^2)	A	B	λ_1^q (10^{-3} GeV^2)	λ_2^g (10^{-3} GeV^2)	λ_3^g (10^{-3} GeV^2)
fit	4.68	1.14	0.50	2.79	1.33	0.36
lattice QCD and QCD sum rules	5.0 ± 0.5	[0.85, 0.95]	[0.23, 0.33]	2.6 ± 1.2	2.3 ± 0.7	0.54 ± 0.2

TABLE I: Comparison between the fit results of this work and the lattice results [57, 58] for the coefficients of the twist-three DA in Eq. (45), parametrizing the $3q$ LFWAs, and the QCD sum rules estimates [41] of the coefficients of the twist-four DAs in Eqs. (46)-(48), parametrizing the $3q + g$ LFWAs.

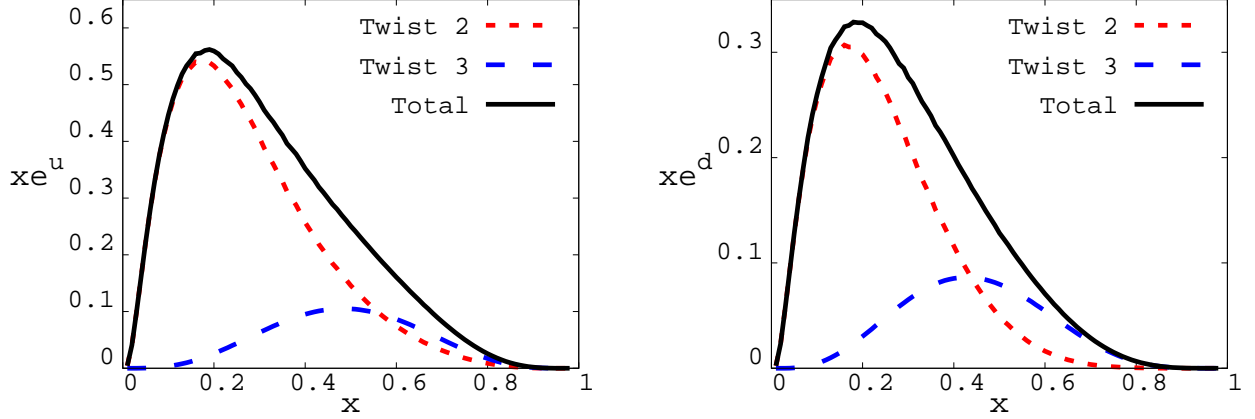


FIG. 2: Results for the PDF $xe^q(x)$ as function of x for the up (left panel) and down (right panel) quark. Red short-dashed curve: twist-two contribution; blue long-dashed curve: pure twist-three contribution; solid curve: total results, sum of the twist-two and twist-three contributions.

quarks. On the other side, the $x\bar{e}^q(x)$ contribution is peaked at $x \approx 0.5$, and becomes the dominant contribution at larger x , especially for down quarks. We also note that the pure twist-3 contributions for the up and down quarks have very similar size, whereas the twist-2 contribution for the up quark is approximately twice as large as the twist-2 contribution for the down quark (note the different scales on the vertical axis).

Recently, the CLAS collaboration has reported preliminary results of a measurement of the beam asymmetry in di-hadron SIDIS, using a longitudinally polarized 6 GeV electron beam off an unpolarized proton target [10, 59]. These data have been analyzed to extract the following flavor combination of the valence-quark contributions to $e^q(x)$:

$$e^V(x) = \frac{4}{9}e^{u_v}(x) - \frac{1}{9}e^{d_v}(x). \quad (56)$$

In Fig. 3, the preliminary CLAS data points at the scale $Q^2 = 1.5 \text{ GeV}^2$ are compared with our model predictions at the scale $Q^2 = 1 \text{ GeV}^2$. The model results are also split in the contributions from twist-two and genuine twist 3-terms, corresponding to the short-dashed blue curve and the long-dashed cyan curve, respectively. Our results are in quite good agreement with the experimental extraction at the two higher- x bins, but they are not able to reproduce the observed fast rising at lower x . This could be due to a lack of our model, that, according to the fit results for the unpolarized PDF f_1 , shown in Fig. 1, is less reliable in the lower- x region. We also notice that the genuine twist-three contribution in the considered x -range is very small, supporting the results within the light-front constituent-quark picture that was used in Ref. [21] and showed to be able to reproduce the results of the CLAS data at higher x . However, one should bear in mind that these data are still preliminary and have unestimated systematic uncertainties.

C. Transverse momentum

Next, we turn our attention to the k_\perp dependence of the TMDs. We define the x -dependent mean squared transverse momentum of a generic TMD $j(x, k_\perp)$ as follows

$$\langle k_\perp^2 \rangle_j(x) = \frac{\int d\mathbf{k}_\perp k_\perp^2 j(x, k_\perp)}{\int dx d\mathbf{k}_\perp j(x, k_\perp)}. \quad (57)$$

The corresponding results for the quark and gluon unpolarized distribution $f_1(x, k_\perp)$ and for the quark TMD $\tilde{e}(x, k_\perp)$ are shown in the left and right panel of Fig. 4, respectively. The quark results refer to the valence-quark contribution, since in our model we neglect the sea quarks. The results for the gluon are obtained from the $3q + g$ component of the proton LFWF, and therefore correspond to the intrinsic non-perturbative gluon contribution. All the results refer to the model scale of $Q^2 = 1 \text{ GeV}^2$. We find that in the case of f_1 , the size and the x -dependence is very similar for up

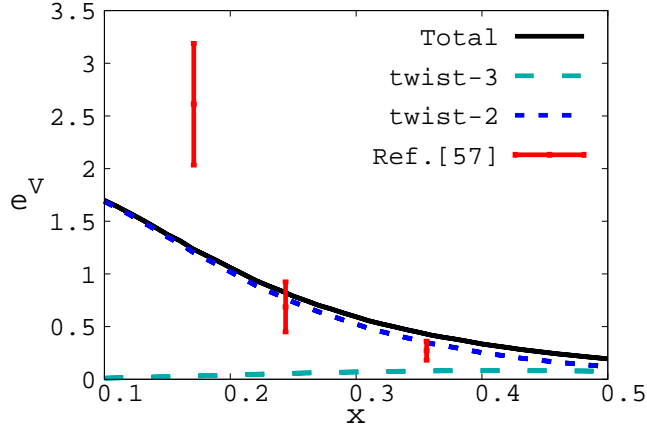


FIG. 3: Predictions for the combination $e^V = \frac{4}{9}e^u(x) - \frac{1}{9}e^d(x)$ at the scale $Q^2 = 1 \text{ GeV}^2$, in comparison with the extraction of Ref. [59] at the scale $Q^2 = 1.5 \text{ GeV}^2$. The dashed curve shows the contribution of the twist-two term of e , and the solid curve corresponds to the total contribution from the sum of the twist-two and twist-three terms of e .

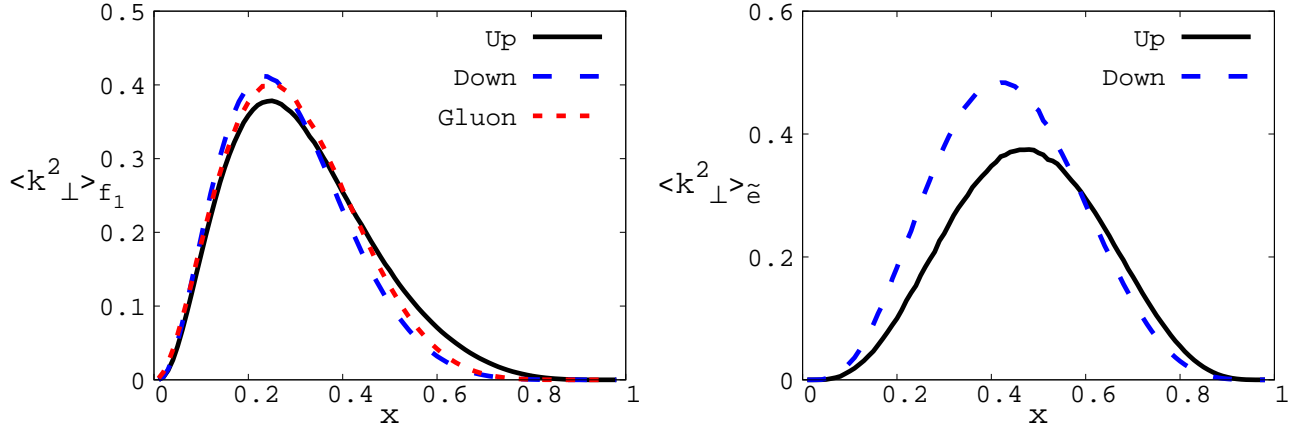


FIG. 4: Results for the x -dependence of the mean squared transverse momentum in Eq. (57) of the unpolarized TMD f_1 (right panel) and the TMD \tilde{e} (left panel) at the model scale of $Q^2 = 1 \text{ GeV}^2$. The solid black curves and the long-dashed blue curves correspond to the up and down quark contributions, respectively, while the long-dashed red curve in the case of f_1 shows the gluon contribution.

and down quarks, and for gluons. They are all peaked at $x \approx 0.3$, and fall down rapidly at higher x , with a very similar slope in the case of the down quarks and the gluon. The similar behavior for down quark and gluons is an indication that the results for the down quark contribution to the f_1 TMD are more dominated by the $3q + g$ component of the LFWF than in the case of up quark. For the quark contribution, there exists a recent extraction, based on a fit of the unpolarized TMD $f_1(x, k_{\perp})$ to available experimental data measured in SIDIS, Drell-Yan and Z boson production [60]. This extraction assumes no quark-flavour dependence and uses data in the range of $5 \cdot 10^{-2} \leq x \leq 0.4$. Therefore, the corresponding results for the mean squared transverse momentum get a sizeable contribution from sea-quarks, which results in a x -dependence quite different from the bell-shaped structure we find in our calculation. Nevertheless, we find that our results are in the same range of values as the phenomenological extraction.

In the case of the mean squared transverse momenta of $\tilde{e}^q(x, k_{\perp})$ we observe a more pronounced quark flavor dependence w.r.t. to the case of the unpolarized twist-two TMD. Furthermore, they are peaked at higher- x values, with the contribution from up quarks slightly shifted at larger x w.r.t. to the one from down quarks.

By integrating Eq. (57) over x , we obtain the results for the $\langle k_{\perp}^2 \rangle$ width of the TMDs. The results for f_1 and \tilde{e} at the model scale of $Q^2 = 1 \text{ GeV}^2$ are presented in Table II. They are very similar for all the partons in the case of f_1 ,

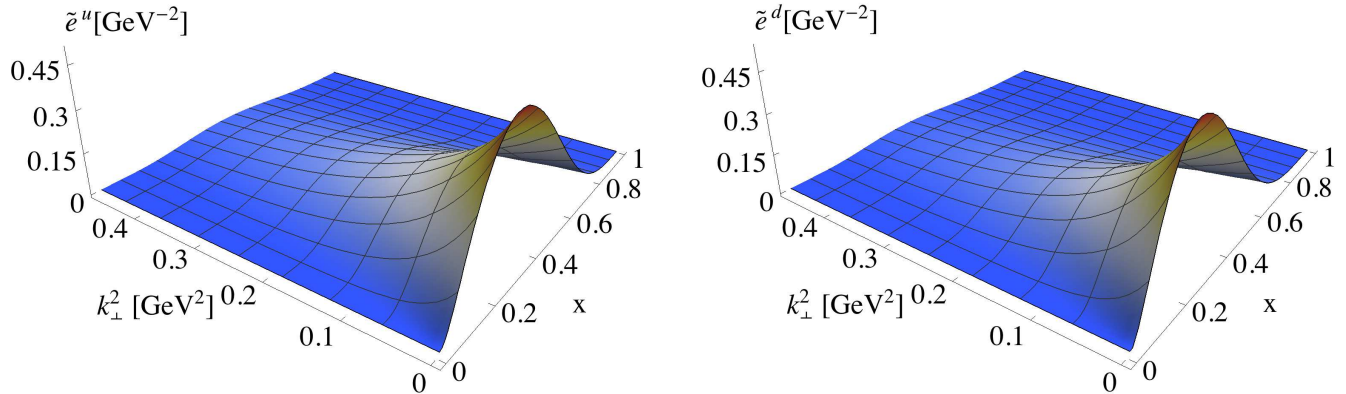


FIG. 5: \tilde{e} for the up (left panel) and down (right panel) quark as a function of x and k_\perp^2 .

while they have an appreciable quark-flavor dependence in the case of \tilde{e} . We also notice the broader widths for the \tilde{e} distribution with respect to f_1 .

	f_1			\tilde{e}	
	u	d	g	u	d
$\langle k_\perp^2 \rangle$ (GeV 2)	0.138	0.133	0.136	0.158	0.196

TABLE II: Results for $\langle k_\perp^2 \rangle$ of the f_1 and \tilde{e} TMDs at $Q^2 = 1$ GeV 2 .

Finally, in Fig. 5 we show the three-dimensional plots of \tilde{e} for the up and down quark, as function of x and k_\perp^2 . For both quark flavors, the k_\perp^2 -dependence of the distributions slightly moves away from a Gaussian shape, as expected from our model Ansatz for the k_\perp^2 -dependence of the LFWFs in Eq. (49).

Conclusions

In this work, we studied the sub-leading structure function e^q .

First, we reviewed its model-independent decomposition, which follows from the QCD EOM. In particular, this decomposition contains a genuine twist-three part, i.e. the “tilde” term encoding the quark-gluon correlations, a pure twist-two contribution and a singular (δ -like) term. The singular term is in turn given by a well-know contribution that can be related to the pion-nucleon-sigma term, and an additional term that, instead, is poorly discussed in literature and has been written down explicitly here for the first time.

Then, we focused on the modeling of the tilde term. To this aim, we constructed a model-independent representation in terms of overlap of LFWFs for the $3q$ and $3q + g$ Fock-components of the proton state. For the calculation, we restricted ourselves to the LFWFs corresponding to zero orbital angular momentum of the partons. This allowed us to relate the $3q$ and the $3q + g$ LFWFs in the limit of zero-transverse separation to the leading-twist and next-to-leading-twist DAs of the proton, respectively. The transverse-momentum dependence of the LFWFs was built up by assuming a modified Gaussian Ansatz, with explicit dependence on the mass of the partons. The DAs and the transverse-momentum dependent part were parametrized in such a way to reproduce available phenomenological parametrizations for the unpolarized PDF f_1 of quarks and gluons at the scale of $Q^2 = 1$ GeV 2 . The fit gave values for the parametrization of the DAs that are consistent with lattice calculations [57, 58] and predictions from QCD sum rules [41].

With these ingredients, we provided predictions for both the quark PDF $\tilde{e}^q(x)$ and the quark TMD $\tilde{e}^q(x, k_\perp)$, in comparison with the corresponding twist-two contribution given in terms of f_1^q . In the case of $\tilde{e}^q(x)$, we found that the pure twist-three contribution has a distinctive x -dependence from the twist-two contribution, and is about 20-30% of the twist-two contribution at the peak position, using our model-results for the quark masses. We also

considered preliminary results from a phenomenological extraction of a particular flavor combination of the valence-quark contribution to $e^q(x)$ [59]. For this quark-flavor combination, our model predictions are almost saturated by the twist-two contribution to $e^q(x)$, and showed a quite good agreement with the extracted results in the large x -region.

The results of this work are encouraging for an extension to other subleading-twist TMDs. However, twist-three TMDs other than e^q involve a transfer of orbital angular momentum between the initial and final proton states. This requires the modeling of the LFWF components with non-zero orbital angular momentum. Work in this direction is in progress.

Acknowledgments

The authors are grateful to A. Bacchetta, V. Braun, C. Lorcé, and P. Schweitzer for stimulating discussions, and to T. Liu for helpful advices in using the phenomenological parametrizations of PDFs. This work is partially supported by the European Research Council (ERC) under the European Union's Horizon 2020 research and innovation programme (grant agreement No. 647981, 3DSPIN).

Appendix A

In this appendix, we show the derivation of the contributions e_m^q in Eq. (15) and $e_{\text{tw}3}^q$ in Eq. (17).

We start by considering the matrix elements of the operators \mathcal{O}_m and $\mathcal{O}_{\text{tw}3}$ in Eqs. (12) and (13), respectively, which enter the definition (4) of the TMD e^q :

$$\int \frac{dz^- d\mathbf{z}_\perp}{(2\pi)^3} e^{iz^- xP^+ - i\mathbf{z}_\perp \cdot \mathbf{k}_\perp} \int_{0^-}^{z^-} d\zeta^- \mathcal{M}_l(\zeta^-, \mathbf{z}_\perp), \quad (l = m, a), \quad (\text{A1})$$

with

$$\mathcal{M}_m(\zeta^-, \mathbf{z}_\perp) := -\frac{im}{2} \langle P | \bar{\psi}(0) \gamma^+ \mathcal{W}_1(0^-, \mathbf{0}_\perp; \zeta^-, \mathbf{z}_\perp) \psi(\zeta^-, \mathbf{z}_\perp) | P \rangle, \quad (\text{A2})$$

$$\begin{aligned} \mathcal{M}_{\text{tw}3}(\zeta^-, \mathbf{z}_\perp) := & \frac{g_s}{2} \left(\int_{\infty^-}^{\zeta^-} d\eta^- \langle P | \bar{\psi}(0) \mathcal{W}_1(0^-, \mathbf{0}_\perp; \eta^-, \mathbf{z}_\perp) G_j^+(\eta^-, \mathbf{z}_\perp) \sigma^{j+} \mathcal{W}_1(\eta^-, \mathbf{z}_\perp; \zeta^-, \mathbf{z}_\perp) \psi(\zeta^-, \mathbf{z}_\perp) | P \rangle \right. \\ & \left. + \int_{0^-}^{\infty^-} d\eta^- \langle P | \bar{\psi}(0) \mathcal{W}_1(0^-, \mathbf{0}_\perp; \eta^-, \mathbf{0}_\perp) G_j^+(\eta^-, \mathbf{0}_\perp) \sigma^{j+} \mathcal{W}_1(\eta^-, \mathbf{0}_\perp; \zeta^-, \mathbf{z}_\perp) \psi(\zeta^-, \mathbf{z}_\perp) | P \rangle \right), \quad (\text{A3}) \end{aligned}$$

where we did not write explicitly $z^+ = 0^+$ in the argument of the fields. By integrating over \mathbf{z}_\perp and introducing the Fourier-transform in the variable ζ^- of the matrix-element \mathcal{M}_l , Eq. (A1) can be rewritten as

$$\int \frac{dz^-}{2\pi} e^{iz^- xP^+} \int_{0^-}^{z^-} d\zeta^- \int dp^+ e^{-i\zeta^- p^+} \mathcal{M}_l(p^+, \mathbf{k}_\perp). \quad (\text{A4})$$

The integral over ζ^- in Eq. (A4) can be easily performed, giving

$$i \int \frac{dz^-}{2\pi} e^{iz^- xP^+} \int dp^+ \frac{e^{-iz^- p^+} - 1}{p^+} \mathcal{M}_l(p^+, \mathbf{k}_\perp). \quad (\text{A5})$$

Finally, integrating Eq. (A5) over z^- and changing the integration variable as $p^+ = yP^+$, we obtain

$$\frac{i}{xP^+} \mathcal{M}_l(xP^+, \mathbf{k}_\perp) - \delta(x) \frac{i}{P^+} \int dy \frac{1}{y} \mathcal{M}_l(yP^+, \mathbf{k}_\perp). \quad (\text{A6})$$

Eq. (A6), for $l = m$ and with the definition (3) for f_1^q , corresponds to the contribution e_m^q in Eq. (15). Analogously, Eq. (A6), for the matrix element with $l = \text{tw}3$, and with the definition (4) for \tilde{e}^q , gives the contribution $e_{\text{tw}3}^q$ in Eq. (17).

Appendix B

The overlap representation of the $\tilde{e}^q(x, k_\perp)$ TMD in terms of the LFWAs corresponding to the parton configuration with zero partons' orbital angular momentum reads

$$\begin{aligned}
\tilde{e}^u(x, k_\perp) = & \frac{4g_s}{Mx\sqrt{3}} \int \frac{[dx]_{1234}[dk]_{1234}}{\sqrt{x_4}} \left\{ -\delta(x - x_4 - x_1)\delta^2(\mathbf{k}_\perp - \mathbf{k}_{\perp 4} - \mathbf{k}_{\perp 1}) \right. \\
& \times \left[\left(4\Psi^{(0)*}(-2 - 3, 3, 2) + 2\Psi^{(0)*}(2, 3, -2 - 3) \right) \Psi^{1\uparrow}(1, 2, 3, 4) \right. \\
& + \left(2\Psi^{(0)*}(-2 - 3, 2, 3) + \Psi^{(0)*}(3, 2, -2 - 3) \right) \Psi^{2\uparrow}(1, 2, 3, 4) \\
& \left. \left. - 2\Psi^{(0)*}(2, -2 - 3, 3) \Psi^\downarrow(1, 2, 3, 4) \right] \right. \\
& + \delta(x - x_4 - x_2)\delta^2(\mathbf{k}_\perp - \mathbf{k}_{\perp 4} - \mathbf{k}_{\perp 2}) \\
& \times \left[2\Psi^{(0)*}(-1 - 3, 1, 3) \Psi^{2\uparrow}(1, 2, 3, 4) - \Psi^{(0)*}(1, -1 - 3, 3) \Psi^\downarrow(1, 2, 3, 4) \right] \\
& \left. + \delta(x - x_4 - x_3)\delta^2(\mathbf{k}_\perp - \mathbf{k}_{\perp 4} - \mathbf{k}_{\perp 3}) \Psi^{(0)*}(-1 - 2, 1, 2) \Psi^{1\uparrow}(1, 2, 3, 4) \right\}, \tag{B1}
\end{aligned}$$

for the up quark, and

$$\begin{aligned}
\tilde{e}^d(x, k_\perp) = & -\frac{4g_s}{Mx\sqrt{3}} \int \frac{[dx]_{1234}[dk]_{1234}}{\sqrt{x_4}} \left\{ \delta(x - x_4 - x_2)\delta^2(\mathbf{k}_\perp - \mathbf{k}_{\perp 4} - \mathbf{k}_{\perp 2}) \right. \\
& \times 2\Psi^{(0)*}(3, 1, -1 - 3) \Psi^{2\uparrow}(1, 2, 3, 4) \\
& + \delta(x - x_4 - x_3)\delta^2(\mathbf{k}_\perp - \mathbf{k}_{\perp 4} - \mathbf{k}_{\perp 3}) \\
& \times \left[\Psi^{(0)*}(2, 1, -1 - 2) \Psi^{1\uparrow}(1, 2, 3, 4) \right. \\
& \left. \left. - \left(\Psi^{(0)*}(1, -1 - 2, 2) + \Psi^{(0)*}(2, -1 - 2, 1) \right) \Psi^\downarrow(1, 2, 3, 4) \right] \right\}, \tag{B2}
\end{aligned}$$

for the down quark. By integration of Eqs. (B1) and (B2) over \mathbf{k}_\perp , one obtains also the corresponding results for the PDF $e^q(x)$.

References

-
- [1] R. L. Jaffe, Nucl. Phys. **B229**, 205 (1983).
 - [2] P. J. Mulders and R. D. Tangerman, Nucl. Phys. **B461**, 197 (1996), [Erratum: Nucl. Phys. B484,538(1997)].
 - [3] K. Goeke, A. Metz, and M. Schlegel, Phys. Lett. **B618**, 90 (2005).
 - [4] R. L. Jaffe and X.-D. Ji, Nucl. Phys. **B375**, 527 (1992).
 - [5] R. L. Jaffe and X.-D. Ji, Phys. Rev. Lett. **67**, 552 (1991).
 - [6] A. V. Efremov and P. Schweitzer, J. High Energy Phys. **08**, 006 (2003).
 - [7] M. Burkardt, Phys. Rev. **D88**, 114502 (2013).
 - [8] H. Avakian et al., JLab Experiment E12-06-015 (2008).
 - [9] H. Avakian et al., JLab Experiment E12-06-112 (2006).

- [10] S. Pisano et al., JLab Experiment E12-06-112B/E12-09-008B (2014).
- [11] D. Boer et al. (2011), arXiv:1108.1713 [nucl-th].
- [12] A. Accardi et al., Eur. Phys. J. **A52**, 268 (2016).
- [13] A. Metz and M. Schlegel, Annalen Phys. **13**, 699 (2004).
- [14] S. Wandzura and F. Wilczek, Phys. Lett. **72B**, 195 (1977).
- [15] A. V. Efremov, K. Goeke, and P. Schweitzer, Phys. Rev. **D67**, 114014 (2003).
- [16] A. V. Efremov, K. Goeke, and P. Schweitzer, Phys. Lett. **B522**, 37 (2001), [Erratum: Phys. Lett.B544,389(2002)].
- [17] E. De Sanctis, W. D. Nowak, and K. A. Oganessian, Phys. Lett. **B483**, 69 (2000).
- [18] H. Avakian, A. V. Efremov, K. Goeke, A. Metz, P. Schweitzer, and T. Teckentrup, Phys. Rev. **D77**, 014023 (2008).
- [19] A. I. Signal, Nucl. Phys. **B497**, 415 (1997).
- [20] H. Avakian, A. V. Efremov, P. Schweitzer, and F. Yuan, Phys. Rev. **D81**, 074035 (2010).
- [21] C. Lorcé, B. Pasquini, and P. Schweitzer, J. High Energy Phys. **01**, 103 (2015).
- [22] R. Jakob, P. J. Mulders, and J. Rodrigues, Nucl. Phys. **A626**, 937 (1997).
- [23] Z. Lu and I. Schmidt, Phys. Lett. **B712**, 451 (2012).
- [24] W. Mao and Z. Lu, Eur. Phys. J. **C73**, 2557 (2013).
- [25] W. Mao, Z. Lu, and B.-Q. Ma, Phys. Rev. **D90**, 014048 (2014).
- [26] J. Balla, M. V. Polyakov, and C. Weiss, Nucl. Phys. **B510**, 327 (1998).
- [27] B. Dressler and M. V. Polyakov, Phys. Rev. **D61**, 097501 (2000).
- [28] P. Schweitzer, Phys. Rev. **D67**, 114010 (2003).
- [29] M. Wakamatsu, Phys. Lett. **B653**, 398 (2007).
- [30] M. Wakamatsu and Y. Ohnishi, Phys. Rev. **D67**, 114011 (2003).
- [31] Y. Ohnishi and M. Wakamatsu, Phys. Rev. **D69**, 114002 (2004).
- [32] C. Cebulla, J. Ossmann, P. Schweitzer, and D. Urbano, Acta Phys. Polon. **B39**, 609 (2008).
- [33] M. Burkardt and Y. Koike, Nucl. Phys. **B632**, 311 (2002).
- [34] R. Kundu and A. Metz, Phys. Rev. **D65**, 014009 (2002).
- [35] A. Mukherjee, Phys. Lett. **B687**, 180 (2010).
- [36] A. Accardi, A. Bacchetta, W. Melnitchouk, and M. Schlegel, J. High Energy Phys. **11**, 093 (2009).
- [37] C. Lorcé, B. Pasquini, and P. Schweitzer, Eur. Phys. J. **C76**, 415 (2016).
- [38] M. Diehl, T. Feldmann, R. Jakob, and P. Kroll, Eur. Phys. J. **C8**, 409 (1999).
- [39] C. Lorcé, B. Pasquini, and M. Vanderhaeghen, JHEP **05**, 041 (2011).
- [40] M. Burkardt and B. Pasquini, Eur. Phys. J. **A52**, 161 (2016).
- [41] V. M. Braun, T. Lautenschlager, A. N. Manashov, and B. Pirnay, Phys. Rev. **D83**, 094023 (2011).
- [42] S. J. Brodsky, T. Huang, and P. Lepage, in *Particle and Fields* (edited by Capri, A.Z. and Kamal, A.N. (Plenum, New York), 1983).
- [43] X.-D. Ji, J.-P. Ma, and F. Yuan, Eur. Phys. J. **C33**, 75 (2004).
- [44] L. A. Harland-Lang, A. D. Martin, P. Motylinski, and R. S. Thorne, Eur. Phys. J. **C75**, 204 (2015).
- [45] R. L. Jaffe, in *The spin structure of the nucleon. Proceedings, International School of Nucleon Structure, 1st Course, Erice, Italy, August 3-10, 1995* (1996), pp. 42–129, arXiv:hep-ph/9602236 [hep-ph].
- [46] C. J. Bomhof, P. J. Mulders, and F. Pijlman, Phys. Lett. **B596**, 277 (2004).
- [47] W.-M. Zhang and A. Harindranath, Phys. Rev. **D48**, 4868 (1993).
- [48] W.-M. Zhang and A. Harindranath, Phys. Rev. **D48**, 4881 (1993).
- [49] J. Kodaira and K. Tanaka, Prog. Theor. Phys. **101**, 191 (1999).
- [50] D. Boer, P. J. Mulders, and F. Pijlman, Nucl. Phys. **B667**, 201 (2003).
- [51] A. Bacchetta, M. Diehl, K. Goeke, A. Metz, P. J. Mulders, and M. Schlegel, J. High Energy Phys. **02**, 093 (2007).
- [52] S. J. Brodsky, B. Pasquini, B.-W. Xiao, and F. Yuan, Phys. Lett. **B687**, 327 (2010).
- [53] B. Pasquini, S. Cazzaniga, and S. Boffi, Phys. Rev. **D78**, 034025 (2008).
- [54] X.-D. Ji, J.-P. Ma, and F. Yuan, Nucl. Phys. **B652**, 383 (2003).
- [55] J. Bolz and P. Kroll, Z. Phys. **A356**, 327 (1996).
- [56] V. M. Braun, A. N. Manashov, and J. Rohrwild, Nucl. Phys. **B807**, 89 (2009).
- [57] V. M. Braun et al. (QCDSF), Phys. Rev. **D79**, 034504 (2009).
- [58] V. M. Braun et al. (QCDSF), PoS **LATTICE2010**, 158 (2010).
- [59] A. Courtoy, arXiv:1405.7659 (2014).
- [60] A. Bacchetta, F. Delcarro, C. Pisano, M. Radici, and A. Signori, J. High Energy Phys. **06**, 081 (2017).